Sharing Traffic Priorities via Cyber–Physical–Social Intelligence: A Lane-Free Autonomous Intersection Management Method in Metaverse

Bai Li, *Member, IEEE*, Dongpu Cao, Shiqi Tang, Tantan Zhang, Hairong Dong, *Senior Member, IEEE*, Yaonan Wang, *Fellow, IEEE*, and Fei-Yue Wang, *Fellow, IEEE*

***Abstract*—Replacing traffic signals with roadside vehicle-to-infrastructure systems in the era of connected and autonomous vehicles (CAVs) is promising. Managing CAVs in a signal-free intersection, known as autonomous intersection management (AIM), controls the driving behavior of each intersection-traverse CAV to maximize the throughput. Although AIM improves the gross throughput, the fairness of each individual vehicle in its right of way is not seriously considered. This study sets up an AIM system in the cyber–physical–social space to trade traverse priorities quantitatively and fairly. To that end, one needs an AIM method that is optimal and stable, otherwise no convincing trades of traverse priorities could be made. This study proposes a near-optimal lane-free AIM method based on numerical optimal control, wherein log-exp functions are deployed to convexify nondifferentiable collision-avoidance constraints. Besides that, a parameterized social force model (SFM) is proposed to provide a tunable initial guess for numerical optimal control. By tuning the urgency weights in SFM, one may get cooperative trajectories in different homotopy classes, which are further utilized to decide the amount of virtual currency to reward those CAVs who tend to share their traverse priorities. The overall method improves the traverse throughput with individual fairness respected. In experiencing this system, passengers learn how to behave with politeness when they drive manually. Experiments show the efficiency and robustness of the AIM method and also show the efficacy of the overall priority-sharing system.**

***Index Terms*—Autonomous intersection management (AIM), cyber–physical–social intelligence, metaverse, numerical optimal control.**

Manuscript received 30 October 2022; accepted 25 November 2022. This work was supported in part by the Fundamental Research Funds for the Central Universities under Grant 531118010509; in part by the National Natural Science Foundation of China under Grant 62103139; in part by the Natural Science Foundation of Hunan Province, China, under Grant 2021JJ40114; and in part by the 2022 Opening Foundation of State Key Laboratory of Management and Control for Complex Systems under Grant E2S9021119. This article was recommended by Associate Editor Y. Tang. *(Corresponding author: Dongpu Cao.)*

Bai Li is with the State Key Laboratory of Advanced Design and Manufacturing for Vehicle Body and the College of Mechanical and Vehicle Engineering, Hunan University, Changsha 410082, China (e-mail: libai@zju.edu.cn).

Dongpu Cao is with the School of Vehicle and Mobility, Tsinghua University, Beijing 100084, China (e-mail: dongpu.cao@uwaterloo.ca).

Shiqi Tang and Tantan Zhang are with the College of Mechanical and Vehicle Engineering, Hunan University, Changsha 410082, China (e-mail: tangshiqi@hnu.edu.cn; zhangtantan@hnu.edu.cn).

Hairong Dong is with the School of Electronics and Information Engineering, Beihang University, Beijing 100191, China (e-mail: hrdong@bjtu.edu.cn).

Yaonan Wang is with the College of Electrical and Information Engineering and the National Engineering Laboratory for Robot Visual Perception and Control, Hunan University, Changsha 410082, China (e-mail: yaonan@hnu.edu.cn).

Fei-Yue Wang is with the State Key Laboratory for Management and Control of Complex Systems, Institute of Automation, Chinese Academy of Sciences, Beijing 100190, China (e-mail: feiyue@ieee.org).

This article has supplementary material provided by the authors and color versions of one or more figures available at https://doi.org/10.1109/TSMC.2022.3225250, provided by the authors.

Digital Object Identifier 10.1109/TSMC.2022.3225250

I. Introduction

THE NUMBER of passenger cars and commercial vehicles on urban roads has increased rapidly in the past decade, which inevitably causes congestion and numerous accidents [1], [2], [3], [4], [5], [6]. Intersections are the primary source of congestion in an urban transportation system [7], [8], [9]. Traffic signal control and road infrastructure reconstruction are typical approaches for relieving traffic congestion [10]. In contrast to making physical changes to the road layout, traffic signal control is flexible to deal with various traffic densities [11], [12]. The replacement of traffic signals with roadside vehicle-to-infrastructure systems in the era of connected and autonomous vehicles (CAVs) is promising [13]. Managing CAVs in a signal-free intersection, which is also known as autonomous intersection management (AIM), involves controlling the driving behavior of each vehicle when traversing an intersection [14], [15], [16]. AIM can largely promote traffic throughput because most conventional traffic light stops are unnecessary.

Although AIM improves overall traffic throughput at an intersection, the fairness of each individual vehicle in its right of way is ignored. Suppose that two conflicting CAVs simultaneously reach the same spot if they cruise at a nominal speed. The overall throughput will be the same regardless of which CAV yields, but either car has to sacrifice its traverse priority without any reward. An intuitive remedy for this unfairness is to record the yielding/overtaking action and assign a high/low priority next time. A similar idea called congestion pricing has been considered to charge traffic participants for their contributions to congestion [17]. Following this idea, we set up a trading rule for AIM-controlled intersections: if one CAV intends to get a high traverse priority, then it needs to pay those yielding CAVs for the underlying congestion caused to them by some kind of virtual currency. Notably, we assume that the passengers' overtaking/yielding preferences can still

influence the CAVs' driving behaviors [18], [19] although the CAVs drive autonomously in an AIM-controlled intersection. Thus, polite driving behaviors are rewarded quantitatively with virtual currency [20], [21], which is used to purchase a high-priority traverse right for an urgent trip in the future [22], [23]. One may set up a metaverse to fairly evaluate and trade such virtues. Deploying such a metaverse enhances fairness in transportation and improves the politeness of human drivers in real-world society [24], [25]. This study focuses on building an AIM system in a metaverse to trade intersection traverse priorities fairly.

Two technical problems should be resolved in building a priority-sharing AIM system. The first problem is how to measure the behavior quantitatively when a vehicle yields or overtakes its right of way. The second problem is how to maintain a stable traffic order even if an individual is trying to monopolize the right of way. To address the two problems, a fundamental assumption is that the AIM method should be optimal and stable; otherwise, no fairness is achieved to convince the traffic participants. However, as explained in Section II, most of the prevalent AIM methods neither leverage the cooperation potential among vehicles nor fully utilize the spatial space of an intersection zone.

The contributions of this study are threefold. First, a priority-sharing AIM architecture is proposed, which enables buying and selling traverse priorities fairly in an unsignalized intersection. Second, a lane-free AIM method is proposed to quickly find near-optimal cooperative trajectories for traffic flows entering the intersection. Specifically, a novel *log-exp* function is adopted to tractably model the collision-avoidance constraints in the concerned cooperative trajectory planning problem; a social force model (SFM) is adopted to provide tunable initial guesses for warm-starting the numerical optimization process. The tunable initial guesses pave way for our third contribution, which is the proposal of a behavior measurement method, so that yielding or overtaking actions may be fairly traded.

The remaining parts of this article are organized as follows. Section II reviews the existing AIM methods, Section III presents the overall conceptual framework of an urban transportation system in a metaverse, Section IV proposes a fast and near-optimal AIM method that enables lane-free cooperative trajectory planning for CAVs in the intersection, Section V measures the CAVs' driving behaviors so that traverse priorities could be traded, Section VI presents the simulation and experimental results, and Section VII concludes this article.

II. Related Works

The existing AIM methods do not provide high-quality cooperative trajectories for CAVs that traverse an intersection. This limits their applications in a priority-sharing metaverse. Typical drawbacks of previous AIM studies are listed below.

First, collision avoidance operation is overcautious. Dresner and Stone [26] divided an entire intersection zone into tiles and required that different CAVs cannot share common tales at any time. Although checking collisions fast, the tile-occupancy method conservatively takes some free space as the vehicle body. Thus, this method is imprecise, especially when the tile-division resolution is low. Li and Wang [27] proposed a safe pattern that forbids conflicting vehicle types to appear in the intersection simultaneously. This safe pattern is still conservative because it excludes the chances that conflicting types of vehicles coexist in an intersection. Malikopoulos et al. [28], Fayazi and Vahidi [29], Cai et al. [30], Wu et al. [31], Lee and Park [32], and Hadjigeorgiou and Timotheou [33] employed similar strategies to model collision avoidance constraints. Levin and Rey [34] believed that intervehicle collisions occur only at finite conflicting points. But this statement is inaccurate because differences in the CAVs' geometric shapes are ignored.

Second, the vehicle kinematic model is inaccurate. Li et al. [35] defined intersection traverse paths as a combination of line segments and circular curves, which leads to kinematic infeasibility because the curvature of such a traverse path is discontinuous. Although not explicitly presented, most fixed-lane AIM methods suffer from this issue.

Third, intersection-traverse paths are fixed or restricted for selection among finite candidates. Limitations on the traverse paths largely reduce the flexibility and cooperation potential of a CAV team [36], [37]. With fixed traverse paths, the nominal AIM scheme is degraded to how to determine passing order and how to plan vehicle velocities [38]. However, it is possible that two conflicting vehicles have the same passing order if they evade each other by nudging.

Fourth, velocity does not change flexibly when CAVs traverse an intersection. A constant-velocity or constant-acceleration requirement was imposed in [27], [28], [30], [32], [34], and [39], which is conservative and vulnerable to deadlock [15]. Medina et al. [40] determined the longitudinal velocity of each CAV via adaptive cruise control, which makes the velocity planning process partly flexible. Mirheli et al. [41] determined the velocity of each CAV by solving a mixed-integer nonlinear program (NLP), which is also flexible.

Fifth, an AIM method is inapplicable in real time if it involves a heavy computation burden. Taking an intersection zone as a free space, Li and Zhang [42] modeled the AIM task as a cooperative trajectory planning problem in the form of a centralized optimal control problem (OCP) with intractably scaled collision-avoidance constraints. Solving such an OCP numerically is time-consuming. Li et al. [43] proposed a stage division strategy to transfer the online computation burden to building an offline lookup table. However, the creation of a medium-scale lookup table will take years before the AIM method is applicable. Li and Shao [44] pointed out that intervehicle collision-avoidance constraints are the main source of difficulties in dealing with a cooperative trajectory planning problem because they are nonconvex and nondifferentiable. Amouzadi et al. [45] simplified the collision-avoidance constraints in [42] via optimization-based collision avoidance (OBCA) to facilitate the solution process. However, global optimality is not achieved without a high-quality initial guess [46]; the scale of intervehicle collision-avoidance constraints is still intractable, thus, making [45] not fast enough.

TABLE I
PROPERTY ANALYSIS OF EXISTING AIM METHODS

Reference	Is collision avoidance accurate?	Is vehicle kinematics accurate?	Is path flexible?	Is velocity flexible?	Is running in real time?
[27] Li and Wang, 2006	×	√	×	√	√
[26] Dresner and Stone, 2008	×	√	×	×	√
[32] Lee and Park, 2012	×	√	×	×	√
[34] Levin and Rey, 2017	×	√	×	×	√
[40] Medina et al, 2017	√	√	×	√	√
[28] Malikopoulos et al., 2018	×	√	×	×	√
[43] Li, et al., 2018	√	√	√	√	×
[29] Fayazi and Vahidi, 2018	×	√	×	×	√
[39] He et al., 2018	√	√	×	×	√
[41] Mirheli et al., 2019	√	√	×	√	√
[35] Li, et al., 2019	√	×	×	×	×
[45] Amouzadi et al., 2022	√	√	√	√	×
[33] Hadjigeorgiou and Timotheou, 2022	×	√	×	√	√
[30] Cai et al., 2022	×	√	×	×	√
This work	√	√	√	√	√

Table I summarizes the strengths and limitations of typical AIM methods mentioned above. One may notice that no previous studies can provide microscopically optimal AIM solutions in real time. We believe that the output of a qualified AIM method should be optimal; otherwise, no fair measurement of yielding or overtaking motions could be made. The next few sections present our AIM solution, which is near-optimal, fast, and robust.

III. OVERALL FRAMEWORK

The overall working principle of the priority-sharing AIM system in the metaverse is depicted in Fig. 1. The primary procedures of the AIM system work in an event-triggered way [47], [48], which are introduced as follows.

As the first step, each CAV is registered in the AIM system when it reaches a certain range outside the intersection. Right after the registration, the kinematic property, geometric size, driving status, and traverse intention of the CAV are sent to the AIM system via wireless communication.

In the second step, each CAV adjusts its driving status via adaptive cruising control or optimal control to ensure that it drives with a standard longitudinal speed v_{std} along the center of a lane [49].

In the third step, the intersection traverse trajectory of the CAV is planned together with the trajectories of other CAVs in a batch. The AIM reserves an intersection-entrance moment for the CAV, after which the CAV begins to accelerate or decelerate so that it enters the intersection at the assigned moment.

In the fourth step, roadside units collect the closed-loop tracking data of the CAV until it exits the intersection.

Thereafter, the collected data is sent to the central AIM system before a traverse-priority-sharing principle is applied to calculate how each CAV would be rewarded or charged in the fifth step.

In the sixth step, the account balance of each CAV in the metaverse is updated accordingly. After that, the registration of the concerned CAV is canceled in the AIM system. The human driver or the onboard autonomous driving system takes over control of the CAV.

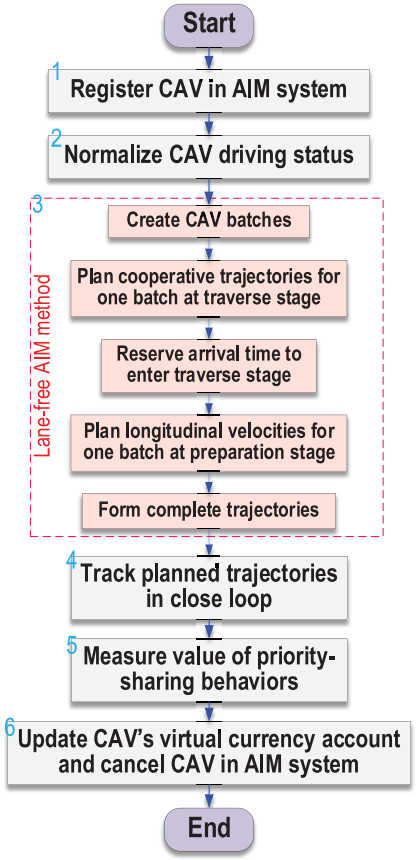

Fig. 1. Overall flowchart of priority-sharing AIM system in the metaverse.

Among the aforementioned steps, step 3 is introduced in Section IV, and step 5 is proposed in Section V.

The aforementioned functions in a priority-sharing AIM metaverse can be realized by constructing a cyber–physical–social space [50], [51], [52], [53], [54], [55], which consists

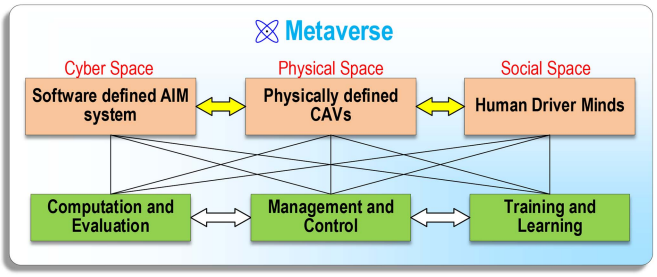

Fig. 2. Schematics on priority-sharing AIM system in the sense of parallel intelligence.

of three modules, namely, artificial societies, computational experiments, and parallel execution (Fig. 2) [56], [57]. Rapid development and long-lasting application of the AIM system in the metaverse would refine the physical, cyber, and social phases of the universe [40].

IV. Lane-Free AIM Method

The nature of AIM is to resolve the spatiotemporal conflicts among the CAVs via cooperative trajectory planning so that the limited space resource in the intersection could be fully used [58]. This section holds several fundamental assumptions about the intersection-traverse CAVs: 1) the CAVs are already registered in the central AIM system; 2) each CAV always keeps good connection with the central AIM system; and 3) each CAV cruises with a standard velocity v_{std} along the centerline of a lane after it completes step 2 mentioned in the preceding section.

For each CAV, the whole intersection-traverse process is divided into three stages, namely, the *preparation stage*, *traverse stage*, and *cruise stage*. The preparation stage refers to the period before the CAV enters the intersection, during which only longitudinal acceleration or deceleration is allowed without any lateral offset. At the traverse stage, the CAV runs in cooperation with other colleagues in a batch. After the traverse stage, the CAV continues to move on with a constant velocity v_{std} at the cruise stage until it is outside the range of the AIM-control region. Fig. 3 takes a left-turn CAV as an example to present the stage division principle of our AIM system. Note that the switching point from the preparation stage to the traverse stage is not the intersection entrance marked with a black dash line in Fig. 3. Similarly, the switching point from the traverse stage to the cruise stage is not the intersection exit (see the solid line in Fig. 3) either. This indicates that the spots to switch between stages are determined flexibly, the technical details of which are presented in the next few sections.

A. Batch Creation

All of the registered CAVs that run stably at the speed of v_{std} are divided into sequential batches. At the preparation stage, the CAVs within one batch always have the same driving status, i.e., they accelerate or decelerate at the same pace so that their velocities are always consistent. The consistent-velocity condition ensures that the relative formation of one batch never alters during the preparation stage. As we introduced later, this

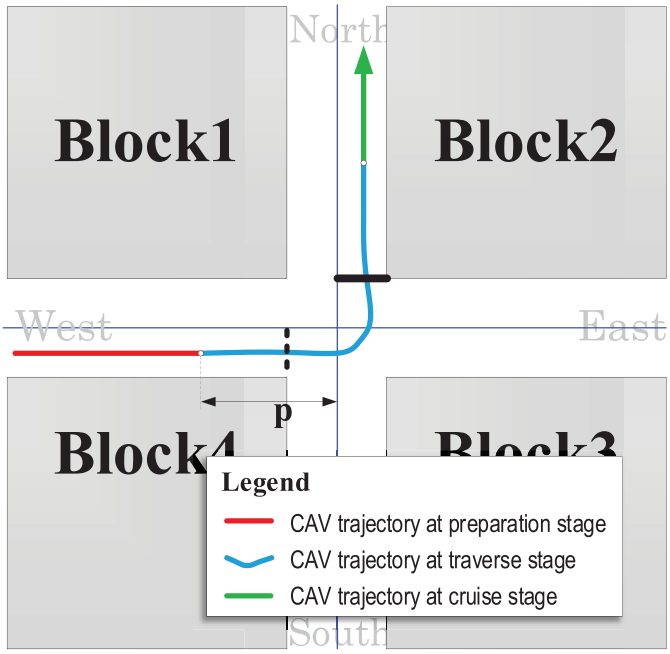

Fig. 3. Schematics on intersection layout and traverse stage division.

property is useful for cooperative trajectory planning at the traverse stage.

Each CAV is not assigned to any specific batch when it has just completed the registration. At a certain frequency, the AIM system collects the status of those CAVs who are not assigned to batches, ranks them according to their longitudinal distances to the intersection entrance, and N_{batch} CAVs are clustered into a batch at most, provided that the longest headway within the batch does not exceed s_{batch}.

Let us now define the end of the preparation stage, which is also the beginning of the traverse stage. The terminal moment of the preparation stage is when the leading CAV in the batch touches the extended barrier of the intersection. Herein, the extended barriers refer to the red dashed lines in Fig. 4, which are biased from the intersection center by L_{ext}. Compared to the real barriers of the $L_{\text{real}} \times L_{\text{real}}$ intersection zone (marked by green lines in Fig. 4), the extended barriers enable the CAVs to anticipate the traditional human-driven vehicles so that better cooperation may be leveraged during the entire intersection-traverse process. It is also required that each batch terminates the preparation stage with a standard status, i.e., each vehicle drives in the centerline of its current lane at a longitudinal speed of v_{std} and a null acceleration. In this way, the traverse stage becomes independent from the preceding preparation stage because the traverse stage begins with a standard status.

Although the boundary status of the batch is standard, it is still unknown when a batch terminates the preparation stage. Let us leave this problem to Section IV-C, before which we focus on how to identify cooperative trajectories at the traverse stage.

B. Cooperative Trajectory Planning

This section introduces how one batch of CAVs passes the intersection at the traverse stage. This is achieved by

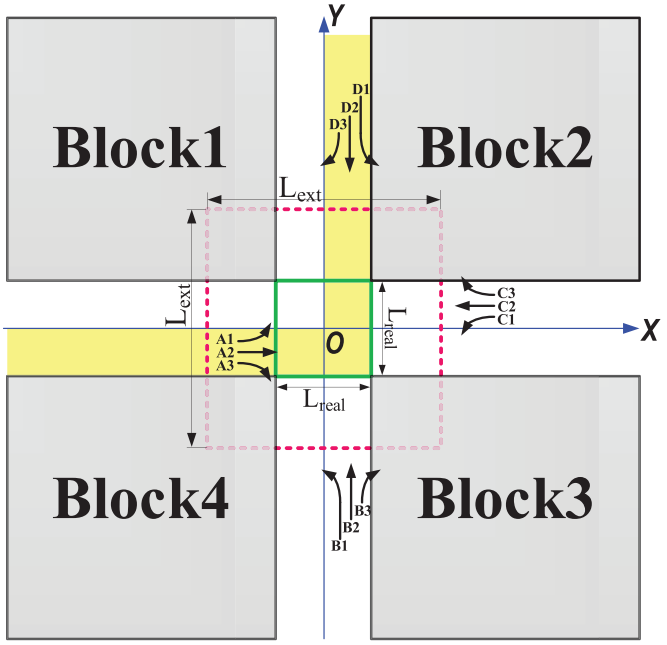

Fig. 4. Schematics on intersection geometric size, coordination frame, and CAV types.

formulating a cooperative trajectory planning problem and solving it numerically. Notably, we are still unsure about the exact time that the batch enters the traverse stage, but the following factors are known for sure. First, the initial boundary values of the CAVs in the batch are explicitly given. Second, the terminal boundary constraints of the CAVs in the batch can be clearly defined. Third, the duration of the traverse stage is fixed as a constant $T_{\text{traverse}} > 0$. Besides that, this section holds an assumption that one batch can safely ignore all other batches when it is at the traverse stage. The three factors and the assumption make the cooperative trajectory planning problem isolated from the entire traffic flow. This renders an interesting result that, trajectory planning at the traverse stage is done before that of the preparation stage. It deserves to explain that the assumption to ignore interbatch collisions is reasonable due to our algorithm design in the next section. The remaining of this section is focused on how to plan cooperative trajectories for one batch at the traverse stage.

An OCP is formulated to describe the concerned cooperative trajectory planning scheme. Recall that the number of CAVs in one batch is restricted by both N_{batch} and s_{batch}. The number of CAVs in the current batch is denoted as N_V without loss of generality. The OCP consists of a cost function and constraints, which include the kinematic constraints, two-point boundary constraints, and collision-avoidance constraints. The details of the OCP are presented as follows.

Kinematic Constraints in the OCP: The kinematic principle of each CAV is known as nonholonomic [59], [60], [61], [62], [63]. A common approach to describe the nonholonomic feature of vehicle kinematics is a single-track bicycle model, which is accurate when a CAV runs at not-too-high speeds without side slips [64], [65]. As a basic step, a Cartesian coordinate frame is set up with the intersection center taken as the original point (Fig. 4). Following this, we have

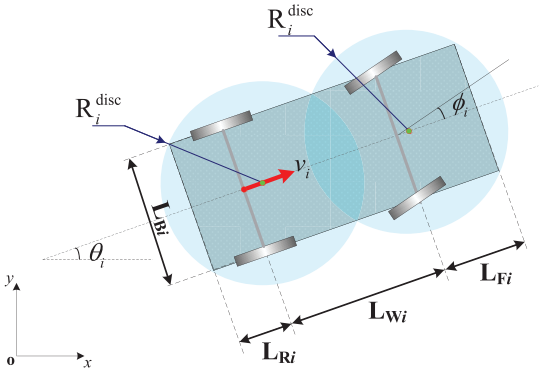

Fig. 5. Schematics on two discs to cover the rectangular body of a CAV.

$$\frac{d}{dt}\begin{bmatrix} x_i(t) \\ y_i(t) \\ v_i(t) \\ \phi_i(t) \\ \theta_i(t) \end{bmatrix} = \begin{bmatrix} v_i(t)\cdot\cos\theta_i(t) \\ v_i(t)\cdot\sin\theta_i(t) \\ a_i(t) \\ \omega_i(t) \\ \frac{v_i(t)\cdot\tan\phi_i(t)}{L_{Wi}} \end{bmatrix}$$
$$i = 1, \ldots, N_V, \ \ t \in [0, T_{\text{traverse}}]. \tag{1}$$

For the ith CAV in the batch, (x_i, y_i) refers to the location of the rear-wheel axle midpoint, $v_i(t)$ denotes the velocity, $a_i(t)$ denotes the acceleration, $\phi_i(t)$ represents the steering-wheel angle, $\omega_i(t)$ represents the rate of the steering angle, $\theta_i(t)$ refers to the orientation angle, and L_{Wi} denotes the wheelbase (Fig. 5). The time horizon $[0, T_{\text{traverse}}]$ indicates that the starting moment of the traverse stage is temporarily set to $t = 0$.

Some state/control are bounded to describe mechanical limits, which are also part of the kinematic constraints

$$\begin{bmatrix} a_{\min i} \\ v_{\min i} \\ -\Omega_{\max i} \\ -\Phi_{\max i} \end{bmatrix} \le \begin{bmatrix} a_i(t) \\ v_i(t) \\ \omega_i(t) \\ \phi_i(t) \end{bmatrix} \le \begin{bmatrix} a_{\max i} \\ v_{\max i} \\ \Omega_{\max i} \\ \Phi_{\max i} \end{bmatrix}$$
$$i = 1, \ldots, N_V, \ \ t \in [0, T_{\text{traverse}}]. \tag{2}$$

Two-Point Boundary Constraints in the OCP: Suppose that CAV i enters the intersection from the west and exits in the north direction (Fig. 3). The two-point boundary constraints for CAV i are defined as

$$\big[x_i(0), y_i(0), \theta_i(0), v_i(0), a_i(0), \phi_i(0), \omega_i(0)\big] = \big[-p, \ -L_{\text{real}}/4, \ 0, \ v_{\text{std}}, \ 0, \ 0, \ 0\big] \tag{3a}$$
$$[\theta_i(T_{\text{traverse}}), v_i(T_{\text{traverse}}), a_i(T_{\text{traverse}}), \phi_i(T_{\text{traverse}}), \omega_i(T_{\text{traverse}})] = \big[\pi/2, \ v_{\text{std}}, \ 0, \ 0, \ 0\big] \tag{3b}$$
$$x_i(T_{\text{traverse}}) = L_{\text{real}}/4 \tag{3c}$$

and

$$y_i(T_{\text{traverse}}) \ge L_{\text{real}}/2. \tag{3d}$$

Here, the parameter p in (3a) refers to the distance marked in Fig. 3. Notably, the initial-time boundary constraint (3a) restricts the CAV configuration to a specific point. By contrast, the end-time boundary constraints (3b)–(3d) confine the CAV configuration to a specific line in the configuration space. Particularly, (3d) means that the rear wheels of CAV i should

leave the intersection zone at $t = T_{\text{traverse}}$ while (3c) means the vehicle drives along the centerline of the target lane.

Generally speaking, there are three directions to leave an intersection (i.e., straight, left turn, and right turn) and four directions to enter an intersection, thus, there are totally 12 types of traverse modes in the intersection, as marked A1, A2, ..., D3 in Fig. 4. The CAV i that we analyze above is in the A1 type. The boundary constraints for the rest 11 types of CAVs can be defined similarly.

Collision-Avoidance Constraints in the OCP: Recall that interbatch collisions are safely ignored, only vehicle-to-barrier collisions and same-batch intervehicle collisions deserve to be considered at the traverse stage.

As a preliminary step to introduce the vehicle-to-barrier collision-avoidance constraints, let us define the drivable area of each CAV in the intersection. For the A1-type CAV i shown in Fig. 3, the drivable area is highlighted yellow in Fig. 4. Nominally, the following expressions guarantee that CAV i does not collide to the drivable area barriers

$$x_i^{\text{FP}}(t) \le L_{\text{real}}/2 \tag{4a}$$
$$y_i^{\text{FP}}(t) \ge -L_{\text{real}}/2 \tag{4b}$$
$$\left(x_i^{\text{FP}}(t) \ge 0\right) \vee \left(y_i^{\text{FP}}(t) \le 0\right) \tag{4c}$$

where $(x_i^{\text{FP}}(t), y_i^{\text{FP}}(t))$ denotes *any* point on the vehicle footprint at time t. However, (4a)–(4c) can hardly be used in practice due to the following two issues. First, (4a)–(4c) need to be imposed on infinite points on the vehicle footprint, which renders intractably scaled constraints. Second, (4c) is a conditional expression, which is nondifferentiable and thus, beyond the capability of a gradient-based numerical OCP solver. To address the first issue, we use two discs to evenly cover the rectangular CAV body (see Fig. 5), then (4a) and (4b) are simplified as

$$\begin{aligned} x_i^{\text{front}}(t) + R_i^{\text{disc}} &\le L_{\text{real}}/2 \\ x_i^{\text{rear}}(t) + R_i^{\text{disc}} &\le L_{\text{real}}/2 \\ y_i^{\text{front}}(t) - R_i^{\text{disc}} &\ge -L_{\text{real}}/2 \\ y_i^{\text{rear}}(t) - R_i^{\text{disc}} &\ge -L_{\text{real}}/2. \end{aligned} \tag{5}$$

Herein, $(x_i^{\text{front}}, y_i^{\text{front}})$ and $(x_i^{\text{rear}}, y_i^{\text{rear}})$ denote the coordinates of the disc centers, respectively. R_i^{disc} is a constant calculated via simple geometric knowledge (details can be found in [46]). To address the second issue, a log-exp function is introduced to approximate (4c)

$$\begin{aligned} y_i^{\text{front}}(t) + R_i^{\text{disc}} &\le \log\left(e^{N_{\text{large}}\cdot x_i^{\text{front}}(t)} + 1\right) \\ y_i^{\text{rear}}(t) + R_i^{\text{disc}} &\le \log\left(e^{N_{\text{large}}\cdot x_i^{\text{rear}}(t)} + 1\right). \end{aligned} \tag{6}$$

$N_{\text{large}} > 0$ is a sufficiently large constant. As opposed to (4c), (6) is sufficiently continuous and tractable. Although the log-exp function renders some errors in approximating (4c), the errors are minor when N_{large} is set large. More importantly, minor violations of the nominal constraint (4c) do not render any real vehicle-to-street-block collisions because the barrier reflected by (4c) is just a virtual boundary inside the intersection. Therefore, we use (5) and (6) to constrain that the A1-type CAV i moves in its drivable region throughout the whole traverse stage. For the rest 11 types of CAVs, the vehicle-to-barrier collision-avoidance constraints are modeled similarly.

Regarding intervehicle collision-avoidance constraints between two vehicles, the dual discs on two CAVs would yield four forms of constraints, which have been well introduced in the previous studies such as [46]. We omit the trivial details in this article.

Cost Function of the OCP: The CAVs are expected to drive smoothly and efficiently during the traverse stage. Herein, the smoothness is achieved by penalizing drastic state changes in the longitudinal and lateral directions. The traverse efficiency encourages each CAV to travel farther in the target lane after leaving the intersection. Therefore, the cost function is defined as a weighted sum

$$\begin{aligned} J = w_{\text{smoothness}} \cdot \sum_{i=1}^{N_V} \left(\int_{\tau=0}^{T_{\text{traverse}}} \left(a_i^2(\tau) + \omega_i^2(\tau)\right) \cdot d\tau \right) \\ - \sum_{i \in A1 \bigcup B2 \bigcup C3} y_i(T_{\text{traverse}}) - \sum_{i \in A2 \bigcup B3 \bigcup D1} x_i(T_{\text{traverse}}) \\ + \sum_{i \in A3 \bigcup C1 \bigcup D2} y_i(T_{\text{traverse}}) + \sum_{i \in B1 \bigcup C2 \bigcup D3} x_i(T_{\text{traverse}}). \end{aligned} \tag{7}$$

With a slight abuse of the notation, $A1, A2, \ldots, D3$ in (7) are index sets that contain the IDs of the corresponding CAV types. $w_{\text{smoothness}}$ is a user-specified weighting parameter that shows the importance to minimize the smoothness term.

Numerical Solution to the OCP: The aforementioned elements form an OCP, the solution to which represents the cooperative trajectories at the traverse stage. Solving this nonconvex OCP analytically is impossible, thus, it is solved numerically instead [66], [67], [68]. Concretely, the OCP is discretized along the time horizon to formulate an NLP, which is thereafter solved by a gradient-based NLP solver.

In the rare event that an NLP solution process fails or does not converge within requested time, we set up a simplified NLP (denoted as $\text{NLP}_{\text{simplified}}$) with no collision-avoidance constraints between two CAVs. If $\text{NLP}_{\text{simplified}}$ is solved successfully, then we check the resultant trajectories to get a maximum number N_{subset} such that CAVs $1, \ldots, N_{\text{subset}}$ are not conflicting; if the simplified NLP solution process still fails, then we temporarily set $N_{\text{batch}} = 1$ and repeat the aforementioned steps.

Initial Guess of Numerical Optimization: It is common knowledge that a gradient-based NLP solution process relies highly on an initial guess. An initial guess is established by sequentially planning the trajectory for each CAV. Herein, one can estimate the moment to exit the intersection for each CAV under the assumption that each CAV cruises at a nominal speed along a predefined Dubins path. All of the CAVs in one batch are ranked by their exit moments in ascending order. For each CAV in the sequence, we coarsely plan a velocity along a predefined Dubins path via dynamic programming (DP) search in a discretized time-station space, during which already planned trajectories are regarded as moving obstacles.

The aforementioned DP-search-based sequential method generates an initial guess to our concerned AIM scheme. However, it is not tunable with respect to various homotopy classes. We would like to introduce a new method to generate tunable initial guesses. Inspired by the conventional SFM proposed for crowd evacuation simulation in a disaster [69], we propose a tunable SFM to coarsely generate an initial guess, wherein the behavior of each CAV (agent) can be easily determined by several parameters. In the SFM, the motion of an agent is influenced by both attractive and repulsive forces. Regarding the attractive force, we predefine a reference line (the aforementioned Dubins path) for attracting each agent; a spot ahead of the agent along the reference line would attract the agent to reach. Potential risks for an agent to collide with obstacles render repulsive forces, wherein static obstacles denote the drivable region barriers, and moving obstacles refer to the other CAVs in the current batch. The maximum allowable moving speed $\bar{v}_i^{\mathrm{SFM}}$ and attractive force magnitude $\mathrm{mag\_att}_i^{\mathrm{SFM}}$ of each agent are user-specified parameters for CAV i, which determine how urgent a CAV desires to traverse the intersection. Nominally, $\bar{v}_i^{\mathrm{SFM}}$ and $\mathrm{mag\_att}_i^{\mathrm{SFM}}$ should be set identically among the CAVs in a batch, while diversified settings would cause yielding or overtaking actions, which are introduced in Section VI.

C. Intersection-Entrance Reservation

The preceding section presents the principle to generate cooperative trajectories at the traverse stage. This section introduces how to identify the exact time for the batch to switch from the preparation stage to the traverse stage.

A reservation operation is conducted for determining the starting time of the traverse stage. Similar to the first-come-first-serve (FCFS) policy in [26], we try to reserve an arrival time for the batch to enter its traverse stage and then check if such a reservation is valid. Herein, a reservation is valid if it is kinematically reachable and does not render any kind of interbatch collisions. By this batch-processing strategy, the overall traffic flow is handled with ease [70]. If a reservation attempt fails, we postpone the arrival time by $\Delta T_{\mathrm{reserve}}$ and try to reserve again until a valid reservation is achieved.

D. Overall AIM Method

This section introduces how the overall AIM method works. For a specified batch of CAVs, the traverse-stage cooperative trajectories are planned by Section IV-B before a valid arrival time of the traverse stage (denoted as T_{arrival}) is reserved by Section IV-C. Thereafter, an energy-optimal linear OCP is numerically solved for the movements of the batch at the preparation stage. The solution to the linear OCP shows how the batch accelerates or decelerates at the preparation stage from $t = 0$ to T_{arrival} so that the leading vehicle in the batch touches the extended region of the intersection at $t = T_{\mathrm{arrival}}$. The validation of the reserved arrival time indicates that the batch will not collide with other batches during its traverse stage, which lasts from $t = T_{\mathrm{arrival}}$ to $T_{\mathrm{arrival}} + T_{\mathrm{traverse}}$. The CAV batch continues to move on after $t = T_{\mathrm{arrival}} + T_{\mathrm{traverse}}$ with a constant speed v_{st} until they are beyond the control range of the AIM system.

As a summary of the whole section, the proposed AIM method regards the continuous traffic flow as batches of CAVs macroscopically and plans optimal trajectories microscopically. In this way, the large-scale CAVs in the traffic flow are safely decoupled without loss of optimality. The proposed method runs fast because interbatch collisions are not constrained in the OCP but are checked repeatedly instead.

V. Quantitative Measurement of Traverse Priorities

This section introduces a method to measure the trade value of cooperative driving behaviors in the sense of AIM. The core idea is to run the proposed AIM method under two series of parametric settings in parallel, compare the traverse time of each individual CAV under the two series, and then assign a bill to each CAV accordingly. The concrete steps are given as follows.

A. Step 1. Driving Urgency Level Setting

A driving urgency level should be set by the passengers offsite before each vehicle departs from home. This study preliminarily makes the level variable (denoted as urg_i) binary. That means the passengers only choose between urgent ($\mathrm{urg}_i = 1$) or not urgent ($\mathrm{urg}_i = 0$).

B. Step 2. AIM Solution in Parallel

After the vehicle enters an AIM-controlled intersection, its traverse trajectory is planned together with its companions in a batch using the nominal method proposed in Section IV, where all the CAVs in a batch share the same setting of $\bar{v}_i^{\mathrm{SFM}}$ or $\mathrm{mag\_att}_i^{\mathrm{SFM}}$. We assume that each CAV can perfectly track the resultant traverse trajectory, then the wall-clock time that each CAV passes the exit barrier of the intersection may be collected and stored in a vector $\zeta_{\mathrm{norm}} = \{T_i^{\mathrm{norm}} | i = 1, \ldots, N_V\}$.

In the meantime, a different scheme is dealt with via parallel computation. Compared with the nominal one, the new AIM scheme is the same except that those CAVs who are marked with $\mathrm{urg}_i = 1$ will have their $\bar{v}_i^{\mathrm{SFM}}$ or $\mathrm{mag\_att}_i^{\mathrm{SFM}}$ settings doubled. Although it appears that urg_i only influences the initial guess generation method (i.e., the tunable SFM), it alters the homotopy class, thereby directly determining which local optimum a numerical optimizer can find. Since the numerical OCP process is not influenced by any urgency-related issue, the resultant traverse trajectories are still kinematically feasible and free from any collision risk. Notably, since the cooperative trajectories at the traverse stage are altered, the trajectories at the preparation stage are likely to be different as well. We collect the planned trajectory for each CAV and store all of the trajectories in a set $\mathrm{Traj}_{\mathrm{new}}$.

C. Step 3. Closed-Loop Tracking Data Collection

The trajectories $\mathrm{Traj}_{\mathrm{new}}$ derived in the preceding step are sent to each CAV for closed-loop tracking control. The actual moment that each vehicle passes the real-world exit line of the intersection is recorded in $\zeta_{\mathrm{real}} = \{T_i^{\mathrm{real}} | i = 1, \ldots, N_V\}$.

D. Step 4. Assign Bills to CAVs

Trades are made by comparing between ζ_{norm} and ζ_{real}. Let us deploy two index sets U and N, which represent the CAV IDs with and without urgent travel demands. Then the gross delayed time of the nonurgent vehicles is

$$\Delta T_{\text{delayed}} = \sum_{i \in N} \left\lfloor T_i^{\text{real}} - T_i^{\text{norm}} \right\rfloor \tag{8}$$

where the operation $\lfloor \quad \rfloor$ is defined as

$$\lfloor x \rfloor = \begin{cases} x, & \text{if } x > 0 \\ 0, & \text{else} \end{cases}. \tag{9}$$

Similarly, the gross saved time of the urgent vehicles is

$$\Delta T_{\text{saved}} = \sum_{i \in U} \left\lfloor T_i^{\text{norm}} - T_i^{\text{real}} \right\rfloor. \tag{10}$$

The vehicles that intend to traverse with urgency should pay for those who yield the right of way. For example, the vehicle $k \in U$, together with other urgent CAVs in the batch, should share the bill because they cause the gross delayed time $\Delta T_{\text{delayed}}$. We require that the to-be-charged bill amount charge_k is in proportion with the saved time an urgent CAV earns, that is

$$\text{charge}_k \propto \Delta T_{\text{delayed}} \cdot \frac{\left\lfloor T_k^{\text{norm}} - T_k^{\text{real}} \right\rfloor}{\Delta T_{\text{saved}}}. \tag{11}$$

Similarly, nonurgent vehicles should be rewarded because they contribute to the gross saved time ΔT_{saved} for those urgent vehicles. We define that the to-be-gained bill amount earning_j for $j \in N$ is

$$\text{earning}_j \propto \Delta T_{\text{saved}} \cdot \frac{\left\lfloor T_j^{\text{real}} - T_j^{\text{norm}} \right\rfloor}{\Delta T_{\text{delayed}}}. \tag{12}$$

Notably, due to the complexity of the lane-free trajectory planning at the traverse stage and the existence of $\lfloor \quad \rfloor$, the gross charge $\sum_{k \in U} \text{charge}_k$ does not necessarily equal to $\sum_{j \in N} \text{earning}_j$, thus, the CAV batch is not playing a zero-sum game.

VI. Experimental Results and Discussions

This section validates the efficacy, efficiency, and robustness of the proposed AIM method via simulations and real-world tests. Typical experimental results are presented at https://www.bilibili.com/video/BV1ye4y1x77J/.

A. Simulation Setup

The proposed method is implemented in the MATLAB + AMPL environment on an i9-9900 CPU with 32 GB RAM that runs at 3.10 × 2 GHz. IPOPT [71] is adopted as the NLP optimizer, where HSL ma27 is chosen as the embedded linear solver. Critical parameters are listed in Table II.

We consider an AIM task that 4000 CAVs will traverse an intersection. For each CAV, the driving directions before and after the traverse are randomly determined under a uniform distribution. The throughput is evaluated by the time consumed for all of the 4000 CAVs to pass the intersection.

TABLE II
Parametric Settings for Simulations

Parameter	Description	Setting
v_{std}	Standard velocity as boundary value at each stage	6.66m/s
N_{batch}	Maximum allowable CAV number in one batch	6
s_{batch}	Longest headway distance allowable in one batch	7.0m
L_{ext}	Length of extended intersection zone	24m
L_{real}	Length of real intersection zone	10m
T_{traverse}	Duration of the traverse stage	5.0s
$\Delta T_{\text{reserve}}$	Additional time between two reservation attempts	0.2s
L_{Wi}	CAV wheelbase	2.800m
L_{Fi}	CAV front-hang length	0.960m
L_{Ri}	CAV rear-hang length	0.929m
L_{Bi}	CAV width	1.942m
$a_{\min i}$, $a_{\max i}$	Minimal and maximum accelerations	-2, 2 m/s^2
$v_{\min i}$, $v_{\max i}$	Minimal and maximum velocities	0, 10 m/s
$\Omega_{\max i}$	Maximum rate of steering angle	0.5 rad/s
$\Phi_{\max i}$	Maximum steering angle	0.7 rad
N_{large}	Sufficiently large constant in (6)	100
$w_{\text{smoothness}}$	Weighting parameter in (7)	10^{-3}

TABLE III
Simulations Under Various Settings of N_{batch}

N_{batch}	Throughput [sec]
1	2630.4
2	2752.4
3	2775.2
4	2722.6
5	2621.8
6	2597.2
8	2580.8

B. On the Efficiency of Lane-Free AIM

The first round of simulations investigates the effects to make the intersection zone lane-free. Let us define a variant of our proposed method, which fixes the paths within the intersection and only plans cooperative velocities for the CAVs in a batch. The throughput derived by this algorithm variant is 2899.2 s while that of our proposed method is 2597.2 s. Thus, setting the intersection to a free space and enabling lane-free traverse would result in a 10.42% decrease in the throughput.

C. On the Efficacy of Batch-Processing Framework

The second round of simulations investigates the performance of our proposed method under different settings of batch scale. By testing under various settings of N_{batch}, the comparative results are reported in Table III.

The case $N_{\text{batch}} = 1$ indicates that each batch contains only one vehicle, which makes the proposed method resemble a traditional reservation-based AIM method. Conversely, setting N_{batch} sufficiently large yields a centralized optimization-based AIM method. As seen from Table III, setting N_{batch} too small would not lead to a good throughput, because cooperation among the vehicles is fully ignored. Setting N_{batch} overly large is effective to achieve good throughput, but

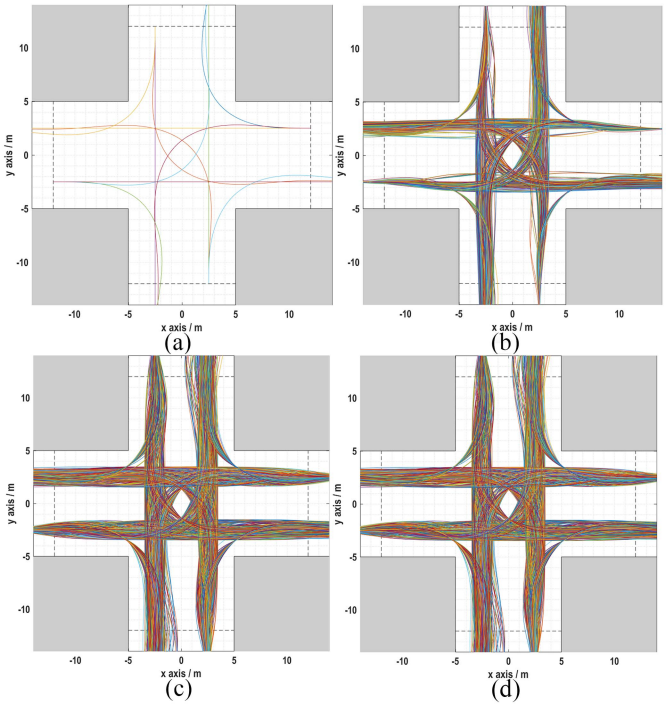

Fig. 6. Footprints of 4000 CAVs' trajectories under (a) $N_{\text{batch}} = 1$; (b) $N_{\text{batch}} = 2$; (c) $N_{\text{batch}} = 6$; and (d) $N_{\text{batch}} = 8$.

cooperative trajectory planning for many CAVs in a batch consumes much. Intuitively, one may expect the throughput to decrease monotonously with the increase in N_{batch}. However, Table III shows that the throughput first increases and then decreases with N_{batch}. The reason behind this interesting result is discussed below.

When the batch scale is small, i.e., $N_{\text{batch}} = 1$, each batch occupies slim intersection space [see Fig. 6(a)], thus, the reserved arrival time of the next batch is not seriously delayed. When the batch scale is large (e.g., $N_{\text{batch}} = 8$), the traverse trajectories within a batch would occupy the entire intersection [Fig. 6(d)], but the gross number of batches is not that much. That is why setting the batch scale limit too large or too small is not bad. However, a medium setting of N_{batch} undertakes the side effects of both ends. Concretely, each batch occupies the majority of an intersection without much cooperation [Fig. 6(b)], thus, making the next batch's reserved arrival time highly delayed. An empirical suggestion is to find the inflection point ($N_{\text{batch}} = 3$ in our simulations) and set N_{batch} larger than that.

Table III also indicates that the effect to reduce the throughput is marginally decreasing when N_{batch} keeps growing. A comparison between Fig. 6(c) and (d) also shows that setting a too large N_{batch} does not contribute obviously to the intersection space utilization.

D. On the Effect of Priority Sharing

This section is focused on the effect of priority sharing when planning cooperative trajectories for a batch of CAVs. The cooperative trajectories of the six CAVs are shown in

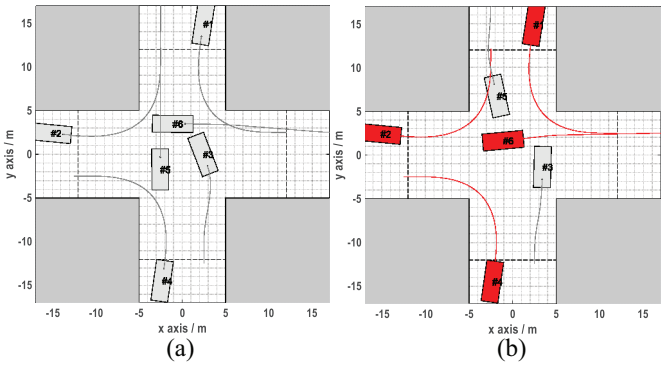

Fig. 7. Comparative simulation results on the effect of priority sharing: (a) none CAVs requests a high priority and (b) four CAVs highlighted in red are requesting a high priority.

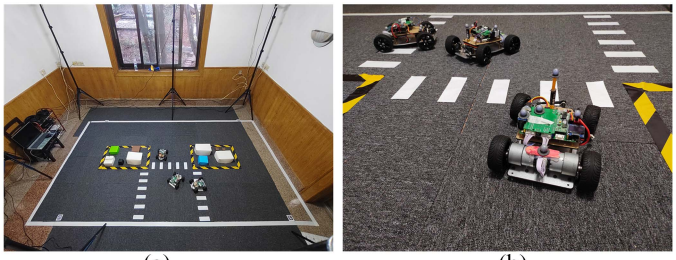

Fig. 8. Set up of indoor field experiments: (a) field layout of a T-junction scenario and (b) reflective marking points on tops of each robot for localization.

Fig. 7(a) when no CAV has requested a high traverse priority. By contrast, the traverse behaviors are slightly different in Fig. 7(b) when four CAVs request a high priority. Concretely, CAV #6 no longer yields to #5 if #6 is urgent. At the same time, the traverse trajectories of CAVs #1, #2, and #4 do not change drastically with/without a high-priority demand, which indicates that the proposed priority-sharing principle maintains the stability of on-road traffic order.

E. Real-World Experiment Setup and Results

Small-scale experiments were conducted with a swarm of three car-like robots in a T-junction scenario [Fig. 8(a)]. The only reason why we built a T-junction rather than an X-junction is that the test field is not wide enough.

Six infrared sensors of NOKOV Motion Capture System were set up for CAV localization. Specifically, reflective marking points were uniquely placed on the top of each car-like robot [Fig. 8(b)]. The reflective marking points reflected the beams emitted from the six light sources before the reflected beams got captured by the infrared sensors. Through this, the position of a robot can be estimated. The localization information was collected on a desktop PC, wherein an AIM system was also implemented. The driving command was sent from the PC to each CAV via ZigBee communication technology. PID was adopted as the longitudinal tracking controller while a pure-pursuit controller is used to minimize lateral offsets.

In a single round of filed test, the three car-like robots ran continuously and stably until the three on-board batteries became low 30 min later. This indicates that the proposed AIM system works efficaciously and robustly.

VII. Conclusion

This article has proposed a lane-free AIM method in the metaverse that supports trading traverse priorities fairly and quantitatively.

Comparative simulations indicate the proposal can reduce the throughput efficiently. The proposed AIM method is even more promising when users can set a larger batch scale without the loss of real-time performance with high-performance CPUs in the future.

The overall idea to set up a priority-sharing AIM system in the metaverse has leveraged the idea of a 6S society in the sense of cyber–physical–social intelligence [72]. Concretely, *safety* in the physical space is ensured by collision-avoidance constraints; *security* in the information space is protected by emerging techniques such as blockchain [73], [74]; *sensitivity* to individual CAV is well respected by our priority-sharing quantification method in Section V; *services* of *smartness* are reflected by the AIM system introduced in Section IV, which tries to reduce the throughput with computational intelligence; *sustainability* is reflected by the robustness of our method, which runs stably even if imbalanced demands about the right of way shall appear; the overall system also tries to influence human drivers indirectly with polite driving preferences and good attitudes in conventional transportation scenarios. In this sense, this article may be regarded as a preliminary step toward the 6S society with concrete implementation principles. Other urban transportation scenarios in the metaverse might be handled similarly.

References

[1] H. Yang, G. Zhai, X. Liu, L. Yang, Y. Liu, and Q. Yuan, "Determinants of city-level private car ownership: Effect of vehicle regulation policies and the relative price," *Transport Policy*, vol. 115, pp. 40–48, Jan. 2022.

[2] X. Xu, L. Zuo, X. Li, L. Qian, J. Ren, and Z. Sun, "A reinforcement learning approach to autonomous decision making of intelligent vehicles on highways," *IEEE Trans. Syst., Man, Cybern., Syst.*, vol. 50, no. 10, pp. 3884–3897, Oct. 2020.

[3] Y. Ma, Z. Wang, H. Yang, and L. Yang, "Artificial intelligence applications in the development of autonomous vehicles: A survey," *IEEE/CAA J. Automatica Sinica*, vol. 7, no. 2, pp. 315–329, Mar. 2020.

[4] Y. Li, G. Yin, W. Zhuang, N. Zhang, J. Wang, and K. Geng, "Compensating delays and noises in motion control of autonomous electric vehicles by using deep learning and unscented Kalman predictor," *IEEE Trans. Syst., Man, Cybern., Syst.*, vol. 50, no. 11, pp. 4326–4338, Nov. 2020.

[5] M. Yue, X. Hou, X. Zhao, and X. Wu, "Robust tube-based model predictive control for lane change maneuver of tractor-trailer vehicles based on a polynomial trajectory," *IEEE Trans. Syst., Man, Cybern., Syst.*, vol. 50, no. 12, pp. 5180–5188, Dec. 2020.

[6] M. Morsali, E. Frisk, and J. Åslund, "Spatio-temporal planning in multi-vehicle scenarios for autonomous vehicle using support vector machines," *IEEE Trans. Intell. Veh.*, vol. 6, no. 4, pp. 611–621, Dec. 2021.

[7] T. Zhang, W. Song, M. Fu, Y. Yang, and M. Wang, "Vehicle motion prediction at intersections based on the turning intention and prior trajectories model," *IEEE/CAA J. Automatica Sinica*, vol. 8, no. 10, pp. 1657–1666, Oct. 2021.

[8] F. Ahmad, S. A. Mahmud, and F. Z. Yousaf, "Shortest processing time scheduling to reduce traffic congestion in dense urban areas," *IEEE Trans. Syst., Man, Cybern., Syst.*, vol. 47, no. 5, pp. 838–855, May 2017.

[9] D. Zhou, Z. Ma, and J. Sun, "Autonomous vehicles' turning motion planning for conflict areas at mixed-flow intersections," *IEEE Trans. Intell. Veh.*, vol. 5, no. 2, pp. 204–216, Jun. 2020.

[10] W. Yue, C. Li, Y. Chen, P. Duan, and G. Mao, "What is the root cause of congestion in urban traffic networks: Road infrastructure or signal control?" *IEEE Trans. Intell. Transp. Syst.*, vol. 23, no. 7, pp. 8662–8679, Jul. 2022.

[11] L. Li, Y. Lv, and F.-Y. Wang, "Traffic signal timing via deep reinforcement learning," *IEEE/CAA J. Automatica Sinica*, vol. 3, no. 3, pp. 247–254, Jul. 2016.

[12] D. Liu, W. Yu, S. Baldi, J. Cao, and W. Huang, "A switching-based adaptive dynamic programming method to optimal traffic signaling," *IEEE Trans. Syst., Man, Cybern., Syst.*, vol. 50, no. 11, pp. 4160–4170, Nov. 2020.

[13] Y. Liu and H. Gao, "Stability, scalability, speedability, and string stability of connected vehicle systems," *IEEE Trans. Syst., Man, Cybern., Syst.*, vol. 52, no. 5, pp. 2819–2832, May 2022.

[14] X. Qian, F. Altché, J. Grégoire, and A. de La Fortelle, "Autonomous intersection management systems: Criteria, implementation and evaluation," *IET Intell. Transport Syst.*, vol. 11, no. 3, pp. 182–189, 2017.

[15] A. Gholamhosseinian and J. Seitz, "A comprehensive survey on cooperative intersection management for heterogeneous connected vehicles," *IEEE Access*, vol. 10, pp. 7937–7972, 2022.

[16] C. Liu, C.-W. Lin, S. Shiraishi, and M. Tomizuka, "Distributed conflict resolution for connected autonomous vehicles," *IEEE Trans. Intell. Veh.*, vol. 3, no. 1, pp. 18–29, Mar. 2018.

[17] M. D. Simoni, K. M. Kockelman, K. M. Gurumurthy, and J. Bischoff, "Congestion pricing in a world of self-driving vehicles: An analysis of different strategies in alternative future scenarios," *Transp. Res. C, Emerg. Technol.*, vol. 98, pp. 167–185, Jan. 2019.

[18] W. Wang et al., "Decision-making in driver-automation shared control: A review and perspectives," *IEEE/CAA J. Automatica Sinica*, vol. 7, no. 5, pp. 1289–1307, Sep. 2020.

[19] X. Wang, X. Zheng, W. Chen, and F.-Y. Wang, "Visual human–computer interactions for intelligent vehicles and intelligent transportation systems: The state of the art and future directions," *IEEE Trans. Syst., Man, Cybern., Syst.*, vol. 51, no. 1, pp. 253–265, Jan. 2021.

[20] S.-M. Park and Y.-G. Kim, "A metaverse: Taxonomy, components, applications, and open challenges," *IEEE Access*, vol. 10, pp. 4209–4251, 2022.

[21] Z. Zhou, B. Wang, M. Dong, and K. Ota, "Secure and efficient vehicle-to-grid energy trading in cyber physical systems: Integration of blockchain and edge computing," *IEEE Trans. Syst., Man, Cybern., Syst.*, vol. 50, no. 1, pp. 43–57, Jan. 2020.

[22] F. Y. Wang, R. Qin, J. Li, Y. Yuan, and X. Wang, "Parallel societies: A computing perspective of social digital twins and virtual–real interactions," *IEEE Trans. Comput. Soc. Syst.*, vol. 7, no. 1, pp. 2–7, Feb. 2020.

[23] D. Pamucar, M. Deveci, I. Gokasar, M. Tavana, and M. Köppen, "A metaverse assessment model for sustainable transportation using ordinal priority approach and Aczel-Alsina norms," *Technol. Forecast. Soc. Change*, vol. 182, Sep. 2022, Art. no. 121778.

[24] Y. Wang et al., "A survey on metaverse: Fundamentals, security, and privacy," *IEEE Commun. Surveys Tuts.*, early access, Sep. 7, 2022, doi: 10.1109/COMST.2022.3202047.

[25] S. E. Bibri and Z. Allam, "The metaverse as a virtual form of data-driven smart cities: The ethics of the hyper-connectivity, datafication, algorithmization, and platformization of urban society," *Comput. Urban Sci.*, vol. 2, no. 1, pp. 1–22, 2022.

[26] K. Dresner and P. Stone, "A multiagent approach to autonomous intersection management," *J. Artif. Intell. Res.*, vol. 31, pp. 591–656, Jan. 2008.

[27] L. Li and F.-Y. Wang, "Cooperative driving at blind crossings using intervehicle communication," *IEEE Trans. Veh. Technol.*, vol. 55, no. 6, pp. 1712–1724, Nov. 2006.

[28] A. A. Malikopoulos, C. G. Cassandras, and Y. J. Zhang, "A decentralized energy-optimal control framework for connected automated vehicles at signal-free intersections," *Automatica*, vol. 93, pp. 244–256, Jul. 2018.

[29] S. A. Fayazi and A. Vahidi, "Mixed-integer linear programming for optimal scheduling of autonomous vehicle intersection crossing," *IEEE Trans. Intell. Veh.*, vol. 3, no. 3, pp. 287–299, Sep. 2018.

[30] M. Cai et al., "Multi-lane unsignalized intersection cooperation with flexible lane direction based on multi-vehicle formation control," *IEEE Trans. Veh. Technol.*, vol. 71, no. 6, pp. 5787–5798, Jun. 2022.

[31] W. Wu, Y. Liu, W. Liu, F. Zhang, V. Dixit, and S. T. Waller, "Autonomous intersection management for connected and automated vehicles: A lane-based method," *IEEE Trans. Intell. Transp. Syst.*, vol. 23, no. 9, pp. 15091–15106, Sep. 2022.

[32] J. Lee and B. Park, "Development and evaluation of a cooperative vehicle intersection control algorithm under the connected vehicles environment," *IEEE Trans. Intell. Transp. Syst.*, vol. 13, no. 1, pp. 81–90, Mar. 2012.

[33] A. Hadjigeorgiou and S. Timotheou, "Real-time optimization of fuel-consumption and travel-time of CAVs for cooperative intersection crossing," *IEEE Trans. Intell. Veh.*, early access, Mar. 15, 2022, doi: 10.1109/TIV.2022.3158887.

[34] M. Levin and D. Rey, "Conflict-point formulation of intersection control for autonomous vehicles," *Transp. Res. C, Emerg. Technol.*, vol. 85, pp. 528–547, Dec. 2017.

[35] Z. Li et al., "Temporal-spatial dimension extension-based intersection control formulation for connected and autonomous vehicle systems," *Transp. Res. C, Emerg. Technol.*, vol. 104, pp. 234–248, Jul. 2019.

[36] G. P. Antonio and C. Maria-Dolores, "Multi-agent deep reinforcement learning to manage connected autonomous vehicles at tomorrow's intersections," *IEEE Trans. Veh. Technol.*, vol. 71, no. 7, pp. 7033–7043, Jul. 2022.

[37] B. Li, Y. Zhang, T. Acarman, Y. Ouyang, C. Yaman, and Y. Wang, "Lane-free autonomous intersection management: A batch-processing framework integrating the reservation-based and planning-based methods," in *Proc. IEEE Int. Conf. Robot. Autom. (ICRA)*, 2021, pp. 7915–7921.

[38] Y. Meng, L. Li, F.-Y. Wang, K. Li, and Z. Li, "Analysis of cooperative driving strategies for nonsignalized intersections," *IEEE Trans. Veh. Technol.*, vol. 67, no. 4, pp. 2900–2911, Apr. 2018.

[39] Z. He, L. Zheng, L. Lu, and W. Guan, "Erasing lane changes from roads: A design of future road intersections," *IEEE Trans. Intell. Veh.*, vol. 3, no. 2, pp. 173–184, Jun. 2018.

[40] A. Medina, N. Van De Wouw, and H. Nijmeijer, "Cooperative intersection control based on virtual platooning," *IEEE Trans. Intell. Transp. Syst.*, vol. 19, no. 6, pp. 1727–1740, Jun. 2018.

[41] A. Mirheli, M. Tajalli, L. Hajibabai, and A. Hajbabaie, "A consensus-based distributed trajectory control in a signal-free intersection," *Transp. Res. C, Emerg. Technol.*, vol. 100, pp. 161–176, Mar. 2019.

[42] B. Li and Y. Zhang, "Fault-tolerant cooperative motion planning of connected and automated vehicles at a signal-free and lane-free intersection," *IFAC-PapersOnLine*, vol. 51, no. 24, pp. 60–67, 2018.

[43] B. Li, Y. Zhang, Y. Zhang, N. Jia, and Y. Ge, "Near-optimal online motion planning of connected and automated vehicles at a signal-free and lane-free intersection," in *Proc. IEEE Intell. Veh. Symp. (IV)*, 2018, pp. 1432–1437.

[44] B. Li and Z. Shao, "A unified motion planning method for parking an autonomous vehicle in the presence of irregularly placed obstacles," *Knowl. Based Syst.*, vol. 86, pp. 11–20, Sep. 2015.

[45] M. Amouzadi, M. O. Orisatoki, and A. M. Dizqah, "Optimal lane-free crossing of CAVs through intersections," *IEEE Trans. Veh. Technol.*, early access, Sep. 15, 2022, doi: 10.1109/TVT.2022.3207054.

[46] B. Li, Y. Ouyang, Y. Zhang, T. Acarman, Q. Kong, and Z. Shao, "Optimal cooperative maneuver planning for multiple nonholonomic robots in a tiny environment via adaptive-scaling constrained optimization," *IEEE Robot. Autom. Lett.*, vol. 6, no. 2, pp. 1511–1518, Apr. 2021.

[47] L. Cao, H. Li, G. Dong, and R. Lu, "Event-triggered control for multiagent systems with sensor faults and input saturation," *IEEE Trans. Syst., Man, Cybern., Syst.*, vol. 51, no. 6, pp. 3855–3866, Jun. 2021.

[48] D. Liu and G.-H. Yang, "A dynamic event-triggered control approach to leader-following consensus for linear multiagent systems," *IEEE Trans. Syst., Man, Cybern., Syst.*, vol. 51, no. 10, pp. 6271–6279, Oct. 2021.

[49] B. Li, Y. Zhang, Y. Feng, Y. Zhang, Y. Ge, and Z. Shao, "Balancing computation speed and quality: A decentralized motion planning method for cooperative lane changes of connected and automated vehicles," *IEEE Trans. Intell. Veh.*, vol. 3, no. 3, pp. 340–350, Sep. 2018.

[50] L. Li, Y. Lin, N. Zheng, and F.-Y. Wang, "Parallel learning: A perspective and a framework," *IEEE/CAA J. Automatica Sinica*, vol. 4, no. 3, pp. 389–395, Jul. 2017.

[51] F.-Y. Wang, N.-N. Zheng, D. Cao, C. M. Martinez, L. Li, and T. Liu, "Parallel driving in CPSS: A unified approach for transport automation and vehicle intelligence," *IEEE/CAA J. Automatica Sinica*, vol. 4, no. 4, pp. 577–587, Sep. 2017.

[52] D. Ding, Q.-L. Han, X. Ge, and J. Wang, "Secure state estimation and control of cyber-physical systems: A survey," *IEEE Trans. Syst., Man, Cybern., Syst.*, vol. 51, no. 1, pp. 176–190, Jan. 2021.

[53] L. Li, L. Lin, D. Cao, Z. Nanning, and W. Feiyue, "Parallel learning—A new framework for machine learning," *ACTA Automatica Sinica*, vol. 43, no. 1, pp. 1–8, 2017.

[54] T. Liu, H. Wang, B. Tian, Y. Ai, and L. Chen, "Parallel distance: A new paradigm of measurement for parallel driving," *IEEE/CAA J. Automatica Sinica*, vol. 7, no. 4, pp. 1169–1178, Jul. 2020.

[55] E. Tunstel et al., "Systems science and engineering research in the context of systems, man, and cybernetics: Recollection, trends, and future directions," *IEEE Trans. Syst., Man, Cybern., Syst.*, vol. 51, no. 1, pp. 5–21, Jan. 2021.

[56] F.-Y. Wang, "Toward a paradigm shift in social computing: The ACP approach," *IEEE Intell. Syst.*, vol. 22, no. 5, pp. 65–67, Sep./Oct. 2007.

[57] F.-Y. Wang, "Parallel intelligence in metaverses: Welcome to Hanoi!" *IEEE Intell. Syst.*, vol. 37, no. 1, pp. 16–20, Jan./Feb. 2022.

[58] B. Liu, Q. Shi, Z. Song, and A. E. Kamel, "Trajectory planning for autonomous intersection management of connected vehicles," *Simul. Model. Pract. Theory*, vol. 90, pp. 16–30, Jan. 2019.

[59] J. Fu, F. Tian, T. Chai, Y. Jiang, Z. Li, and C.-Y. Su, "Motion tracking control design for a class of nonholonomic mobile robot systems," *IEEE Trans. Syst., Man, Cybern., Syst.*, vol. 50, no. 6, pp. 2150–2156, Jun. 2020.

[60] X. Peng, K. Guo, X. Li, and Z. Geng, "Cooperative moving-target enclosing control for multiple nonholonomic vehicles using feedback linearization approach," *IEEE Trans. Syst., Man, Cybern., Syst.*, vol. 51, no. 8, pp. 4929–4935, Aug. 2021.

[61] K. Bergman, O. Ljungqvist, and D. Axehill, "Improved path planning by tightly combining lattice-based path planning and optimal control," *IEEE Trans. Intell. Veh.*, vol. 6, no. 1, pp. 57–66, Mar. 2021.

[62] J. Liu, X. Dong, J. Wang, C. Lu, X. Zhao, and X. Wang, "A novel EPT autonomous motion control framework for an off-axle hitching tractor-trailer system with drawbar," *IEEE Trans. Intell. Veh.*, vol. 6, no. 2, pp. 376–385, Jun. 2021.

[63] Z. Wang, L. Wang, H. Zhang, L. Vlacic, and Q. Chen, "Distributed formation control of nonholonomic wheeled mobile robots subject to longitudinal slippage constraints," *IEEE Trans. Syst., Man, Cybern., Syst.*, vol. 51, no. 5, pp. 2992–3003, May 2021.

[64] K. Majd, M. Razeghi-Jahromi, and A. Homaifar, "A stable analytical solution method for car-like robot trajectory tracking and optimization," *IEEE/CAA J. Automatica Sinica*, vol. 7, no. 1, pp. 39–47, Jan. 2020.

[65] J. K. Subosits and J. C. Gerdes, "Impacts of model fidelity on trajectory optimization for autonomous vehicles in extreme maneuvers," *IEEE Trans. Intell. Veh.*, vol. 6, no. 3, pp. 546–558, Sep. 2021.

[66] B. Li et al., "Optimization-based trajectory planning for autonomous parking with irregularly placed obstacles: A lightweight iterative framework," *IEEE Trans. Intell. Transp. Syst.*, vol. 23, no. 8, pp. 11970–11981, Aug. 2022.

[67] L. Schäfer, S. Manzinger, and M. Althoff, "Computation of solution spaces for optimization-based trajectory planning," *IEEE Trans. Intell. Veh.*, early access, May 18, 2021, doi: 10.1109/TIV.2021.3077702.

[68] B. Li, Y. Ouyang, L. Li, and Y. Zhang, "Autonomous driving on curvy roads without reliance on Frenet frame: A Cartesian-based trajectory planning method," *IEEE Trans. Intell. Transp. Syst.*, vol. 23, no. 9, pp. 15729–15741, Sep. 2022.

[69] D. Helbing and P. Molnar, "Social force model for pedestrian dynamics," *Phys. Rev. E, Stat. Phys. Plasmas Fluids Relat. Interdiscip. Top.*, vol. 51, no. 5, pp. 4282–4286, 1995.

[70] C. Zu, C. Yang, J. Wang, W. Gao, D. Cao, and F.-Y. Wang, "Simulation and field testing of multiple vehicles collision avoidance algorithms," *IEEE/CAA J. Automatica Sinica*, vol. 7, no. 4, pp. 1045–1063, Jul. 2020.

[71] A. Wächter and L. T. Biegler, "On the implementation of an interior-point filter line-search algorithm for large-scale nonlinear programming," *Math. Program.*, vol. 106, no. 1, pp. 25–57, 2006.

[72] D. Cao et al., "Future directions of intelligent vehicles: Potentials, possibilities, and perspectives," *IEEE Trans. Intell. Veh.*, vol. 7, no. 1, pp. 7–10, Mar. 2022.

[73] Y. Wu and J. Dong, "Cyber-physical attacks against state estimators based on a finite frequency approach," *IEEE Trans. Syst., Man, Cybern., Syst.*, vol. 51, no. 2, pp. 864–874, Feb. 2021.

[74] P. Ramanan, D. Li, and N. Gebraeel, "Blockchain-based decentralized replay attack detection for large-scale power systems," *IEEE Trans. Syst., Man, Cybern., Syst.*, vol. 52, no. 8, pp. 4727–4739, Aug. 2022.

Bai Li (Member, IEEE) received the B.S. degree in automation science and electrical engineering from Beihang University, Beijing, China, in 2013, and the Ph.D. degree in control science from Zhejiang University, Hangzhou, China, in 2018.

He is currently an Associate Professor with Hunan University, Changsha, China. He has been the first author of more than 60 journal/conference papers and two books. His research interest is optimization-based motion planning for autonomous driving.

Dr. Li is currently an Associate Editor of IEEE TRANSACTIONS ON INTELLIGENT VEHICLES.

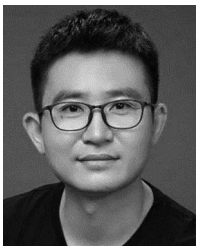

Dongpu Cao received the Ph.D. degree in vehicle dynamics and control from Concordia University, Montreal, QC, Canada, in 2008.

He is a Professor with Tsinghua University, Beijing, China. He has contributed more than 200 papers and three books. His current research interests include driver cognition, automated driving, and cognitive autonomous driving.

Prof. Cao received the SAE Arch T. Colwell Merit Award in 2012 and the IEEE VTS 2020 Best Vehicular Electronics Paper Award and six best paper awards from international conferences. He has served as the Deputy Editor-in-Chief for *IET Intelligent Transport Systems*, and an Associate Editor for IEEE TRANSACTIONS ON VEHICULAR TECHNOLOGY, IEEE TRANSACTIONS ON INTELLIGENT TRANSPORTATION SYSTEMS, IEEE/ASME TRANSACTIONS ON MECHATRONICS, IEEE TRANSACTIONS ON INDUSTRIAL ELECTRONICS, IEEE/CAA JOURNAL OF AUTOMATICA SINICA, IEEE TRANSACTIONS ON COMPUTATIONAL SOCIAL SYSTEMS, and *Journal of Dynamic Systems, Measurement, and Control* (ASME). He is an IEEE VTS Distinguished Lecturer.

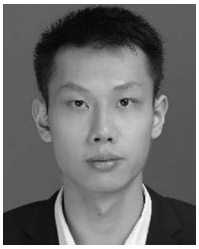

Shiqi Tang received the B.S. degree in mechatronics and control engineering from Wuhan University of Technology, Wuhan, China, in 2020. He is currently pursuing the master's degree in vehicle engineering with the College of Mechanical and Vehicle Engineering, Hunan University, Changsha, China.

His research interests include fail-safe motion planning of an autonomous vehicle system.

Tantan Zhang received the B.S. degree in vehicle engineering from Hunan University, Changsha, China, in 2012, the double M.S. degrees in vehicle engineering from the Politecnico di Torino, Turin, Italy, and Tongji University, Shanghai, China, in 2015, and the Ph.D. degree in energetics from the Politecnico di Torino in 2020.

He is currently an Assistant Professor with the College of Mechanical and Vehicle Engineering, Hunan University. His research interests include motion planning of automated vehicles.

Hairong Dong (Senior Member, IEEE) received the Ph.D. degree in science from Peking University, Beijing, China, in 2002.

She was a Visiting Scholar with the University of Southampton, Southampton, U.K., in 2006 and The University of Hong Kong, Hong Kong, in 2008. She was also a Visiting Professor with the KTH Royal Institute of Technology, Stockholm, Sweden, in 2011. She is currently the Deputy Director of the National Engineering Research Center for Rail Transportation Operation Control System, a Professor with the State Key Laboratory of Rail Traffic Control and Safety, Beijing Jiaotong University, Beijing, and a Professor with Beihang University, Beijing. Her research interests include intelligent transportation systems, automatic train operation, intelligent dispatching, and complex network applications.

Dr. Dong is a Fellow of the Chinese Automation Congress and the Co-Chair of the Technical Committee on Railroad Systems and Applications of the IEEE Intelligent Transportation Systems Society. She serves as an Associate Editor for IEEE TRANSACTIONS ON INTELLIGENT TRANSPORTATION SYSTEMS, IEEE TRANSACTIONS ON INTELLIGENT VEHICLES, *IEEE Intelligent Transportation Systems Magazine*, and *Journal of Intelligent and Robotic Systems*.

Yaonan Wang (Fellow, IEEE) received the B.S. degree in computer engineering from the East China University of Science and Technology, Fuzhou, China, in 1981, and the M.S. and Ph.D. degrees in electrical engineering from Hunan University, Changsha, China, in 1990 and 1994, respectively.

He has been a Professor with Hunan University since 1995. His current research interests include robotics, intelligent perception and control, and computer vision for industrial applications.

Prof. Wang is an Academician of the Chinese Academy of Engineering.

Fei-Yue Wang (Fellow, IEEE) received the Ph.D. degree in computer and systems engineering from Rensselaer Polytechnic Institute, Troy, NY, USA, in 1990.

In 1990, he joined the University of Arizona, Tucson, AZ, USA, where he became a Professor and the Director of Robotics and Automation Laboratory and the Program in Advanced Research for Complex Systems. In 1999, he founded the Intelligent Control and Systems Engineering Center, Institute of Automation, Chinese Academy of Sciences (CAS), Beijing, China, under the support of Outstanding Chinese Talents Program from State Planning Council. In 2002, he was appointed as the Director of the Key Laboratory of Complex Systems and Intelligence Science, CAS, and the Vice President of the Institute of Automation, CAS, in 2006. In 2011, he became the State Specially Appointed Expert and the Founding Director of the State Key Laboratory for Management and Control of Complex Systems. He has been the Chief Judge of Intelligent Vehicles Future Challenge since 2009 and the Director of China Intelligent Vehicles Proving Center with Changshu, since 2015. He is currently the Director of Intel's International Collaborative Research Institute on Parallel Driving with CAS and Tsinghua University, Beijing. His research interests include methods and applications for parallel intelligence, social computing, and knowledge automation.

Dr. Wang was the recipient of the National Prize in Natural Sciences of China, in 2007, numerous best papers awards from IEEE TRANSACTIONS, and became an Outstanding Scientist of ACM for his work in intelligent control and social computing. He was the recipient of IEEE Intelligent Transportation Systems Society outstanding Application and Research Awards in 2009, 2011, and 2015, respectively, the IEEE Systems, Man, and Cybernetics Society Norbert Wiener Award in 2014, and became the IFAC Pavel J. Nowacki Distinguished Lecturer in 2021. Since 1997, he has been the General or Program Chair of more than 30 IEEE, INFORMS, IFAC, ACM, and ASME conferences. He was the President of IEEE Intelligent Transportation Systems Society from 2005 to 2007, IEEE Council of RFID from 2019 to 2021, Chinese Association for Science and Technology, USA, in 2005, American Zhu Kezhen Education Foundation from 2007 to 2008, the Vice President of the ACM China Council from 2010 to 2011, the Vice President and the Secretary General of the Chinese Association of Automation from 2008 to 2018, and the Vice President of IEEE Systems, Man, and Cybernetics Society from 2019 to 2021. He was the Founding Editor-in-Chief (EIC) of the *International Journal of Intelligent Control and Systems* from 1995 to 2000, *IEEE Intelligence Systems Magazine* from 2006 to 2007, IEEE/CAA JOURNAL OF AUTOMATICA SINICA from 2014 to 2017, China's *Journal of Command and Control* from 2015 to 2021, and *Chinese Journal of Intelligent Science and Technology* from 2019 to 2021. He was the EIC of IEEE INTELLIGENT SYSTEMS from 2009 to 2012, IEEE TRANSACTIONS ON INTELLIGENCE TRANSPORTATION SYSTEMS from 2009 to 2016, and IEEE TRANSACTIONS ON COMPUTATIONAL SOCIAL SYSTEMS from 2017 to 2020. He is also the President of CAA's Supervision Council, and the EIC of IEEE TRANSPORTATION ON INTELLIGENCE VEHICLES. He is a Fellow of INCOSE, IFAC, ASME, and AAAS.